



PROPERTIES OF VISCOUS AND JOULEAN DISSIPATION ON FULLY DEVELOPED NATURAL CONVECTION IN A VERTICAL MICRO-CHANNEL IN EXISTENCE OF LORENTZ FORCES.

^{1}Babatunde Aina, ²Sani Isa and ³Deborah Abiola Daramola*

¹Department of Mathematics, Federal University Gashua Nigeria

²Department of Mathematics/Statistics, Yobe State University, Damaturu

³Department of Mathematics, Air Force Institute of Technology, Kaduna

**Corresponding Email: abubakar.im@unilorin.edu.ng*

Manuscript Received: 10/02/2020 Accepted: 07/09/2020 Published: March, 2021

ABSTRACT

Magnetohydrodynamic natural convection flow in a vertical parallel plate micro-channel in presence of viscous and Joulean dissipation is theoretically examined by using a perturbation series method. The effects of velocity slip and temperature jump conditions were taken into consideration. Due to the presence of viscous and Joulean dissipation effects, the momentum and energy equations are coupled system of ordinary differential equations. Roles of Hartmann number, Knudsen number, fluid - wall interaction parameter and dissipation parameter on the flow formation as well as rate of heat transfer are presented. The results revealed that increase in Hartmann number reduced the influence of viscous as well as Joulean dissipation on the velocity, temperature, skin friction and rate of heat transfer. Effect of Hartmann number, rarefaction parameter, fluid wall interaction parameter as well as buoyancy parameter on temperature and velocity is significantly pronounced in the case of symmetric heating.

Keywords: Viscous and Joulean Dissipation; MHD; Natural Convection; Micro-Channel

INTRODUCTION

Magnetohydrodynamic (MHD) phenomenon has received considerable attention during the last two decades owing to its importance in many industrial, technological and the energy generation point of view. Many studies have been conducted on MHD natural convective heat and mass transfer for different physical situation. Nanofluid treatment in a porous enclosure considering thermal non – equilibrium model under the impact of magnetic field has been analyzed by (Sheikholeslami and Shehzad, 2018). (Sheikholeslami and Seyednezhad, 2018) numerically studied Fe304-Ethylene glycol nanofluid electrohydrodynamics flow and natural convection heat transfer in a porous medium. (Sheikholeslami and Moradi, 2018) presented the influence of thermal radiation on nanofluid behaviour in existence of Coulomb forces via CVFEM. (Sheikholeslami, 2018) discussed the Cu0-H20 nanofluid flow in a porous channel with magnetic field using mesoscopic method. Numerical investigation of nanofluid free convection under the influence of electric field in a porous enclosure was carried out by (Sheikholeslami, 2018). Simulation for nanofluid heat transfer in a porous enclosure in presence of thermal radiation and Coulomb force has been investigated by (Sheikholeslami and Rokni, 2018). In another related article, (Sheikholeslami and Shehzad, 2018) presented numerical analysis of Fe304-H20 nanofluid flow in permeable media under the effect of external magnetic source. Influence of magnetic field on nanofluid free convection in an open porous cavity by means of Lattice Boltzmann method has been studied by (Sheikholeslami, 2017). (Sheikholeslami, 2017) presented the influence of a constant magnetic field on the nanofluid natural convection in a porous media with a Sinusoidal hot cylinder. Also, (Sheikholeslami, 2017) investigated the impact of Lorentz forces on magnetic nanofluid free convection in a porous media. (Jha *et al.*, 2015) studied the fully developed steady natural convection flow of conducting fluid in a vertical parallel plate micro-channel in the presence of transverse magnetic field. They discovered that increase of Hartmann number is responsible for decrease in the volume flow rate. The influences of externally applied transverse magnetic field as well as suction/injection on steady natural convection flow of conducting fluid in a vertical micro-channel has been examined by (Jha *et al.*, 2015). They reported that the effect of suction/injection parameter on the micro-channel velocity slip and temperature jump become significant with the decrease of the wall-ambient temperature difference ratio in the absence of induced magnetic field. In another work, (Jha *et al.*, 2016) investigated the role of wall surface curvature on transient MHD free convective flow in vertical micro-concentric-annuli. They concluded that, the slip induced by rarefaction effect and Hartmann number increases as radius ratio increases while

the slip induced by fluid–wall interaction parameter increases as radius ratio decreases. (Jha *et al.*, 2015) studied exact solution of steady fully developed natural convection flow of viscous, incompressible, and electrically conducting fluid in a vertical annular micro-channel. In another related work, (Jha and Aina, 2016) presented the MHD natural convection flow in a vertical micro-porous-annulus (MPA) in the presence of radial magnetic field. It is found that, the rate of heat transfer decreases with increase of fluid-wall interaction parameter in case of suction at outer surface of the inner porous cylinder and injection at inner surface of the outer porous cylinder. The MHD natural convection flow in vertical micro-concentric-annuli (MCA) in the presence of radial magnetic field has been discussed by (Jha *et al.*, 2015). They reported that, as rarefaction parameter increase the velocity slip on the surface of cylinders increases while fluid wall interaction parameter decreases the velocity inside the micro-concentric-annuli. Recently, fully developed natural convection flow in a vertical parallel plate’s micro-channel in the presence of viscous dissipation is theoretically examined by using a perturbation series method by (Jha and Aina, 2018).

However, the earlier work of (Jha and Aina, 2018) considered the effects viscous dissipation, rarefaction and fluid wall interaction on steady natural convection flow in a vertical parallel plate micro-channel, where the effects of Joulean dissipation was not included. Therefore, as a follow- up study of (Jha and Aina, 2018), here, we include the effect of viscous and Joulean dissipation, which is very important at microscale due to the existence of high velocity gradient. To the best of the author’s knowledge, there is no investigation on fully developed natural convection flow in a vertical parallel plate micro-channel in presence of viscous and Joulean dissipation.

MATERIALS AND METHODS

Mathematical Analysis

Steady MHD natural convection flow in a vertical micro-channel formed by two infinitely vertical parallel plates separated by a distance *b* under the effects of viscous and Joulean dissipation is studied as illustrated in Figure 1. The boundary conditions are defined in this figure. The variables are only function of *y* because plates are infinity. The plates are heated asymmetrically with one plate maintained at a temperature *T*₁ where the other plate at temperature *T*₂, where *T*₁ > *T*₂. A uniform magnetic field *B*₀ is passed across the micro-channel normal to the plates and a viscous conducting fluid rises in the micro-channel driven by buoyancy forces and retarded by magnetic forces. Following (Jha *et al.*, 2015) and considering the effects of viscous and Joulean dissipation, under the usual Boussineq approximation and following non dimensional quantities,

$$y = \frac{y}{b}, U = \frac{vu}{g\beta b^2(T_1 - T_0)}, \theta = \frac{T - T_0}{T_1 - T_0}, Pr = \frac{\nu}{\alpha}, M = B_0 b \sqrt{\frac{\sigma}{\rho\nu}} \dots\dots (1)$$

where β is thermal expansion coefficient, T is the temperature, T_0 is the free stream temperature, g is the acceleration due to gravity, ν is the kinematic viscosity of the fluid, μ is the dynamic viscosity and k is thermal conductivity.

The governing equations and boundary conditions can be written in the following dimensionless form:

$$\frac{d^2U}{dY^2} - M^2U + \theta = 0 \tag{2}$$

$$\frac{d^2\theta}{dY^2} + N \left[M^2U^2 + \left(\frac{dU}{dY} \right)^2 \right] = 0 \tag{3}$$

where N is defined [18;19]:

$$N = \rho b^4 g^2 \beta^2 (T_1 - T_0) / (k\nu)$$

with the boundary conditions in non dimensional form as

$$U(Y)=\beta_v Kn \frac{dU}{dY}, \theta(Y)=\xi + \beta_v Kn \ln \frac{d\theta}{dY} \text{ at } Y=0 \tag{4}$$

$$U(Y)=-\beta_v Kn \frac{dU}{dY}, \theta(Y)=1-\beta_v Kn \ln \frac{d\theta}{dY} \text{ at } Y=1$$

$$\beta_v = \frac{2-\sigma_v}{\sigma_v}, \beta_t = \frac{2-\sigma_t}{\sigma_t} \frac{2\gamma_s}{\gamma_s+1} \frac{1}{Pr}, Kn = \frac{\lambda}{b}, \ln = \frac{\beta_t}{\beta_v}, \xi = \frac{T_2 - T_0}{T_1 - T_0}$$

Referring to the values of β_v and β_t given in (Eckert and Drake, 1972) and (Goniak and Duffa, 1995), the value of

β_v is near unity, and the value of β_t ranges from near 1 to more than 100 for actual wall surface conditions and is near 1.667 for many engineering applications, corresponding to

$$\sigma_v = 1, \sigma_t = 1, \gamma_s = 1.4 \text{ and } Pr = 0.71 (\beta_v = 1, \beta_t = 1.667)$$

The physical quantities used in the above equations are defined in the nomenclature.

Method of solution

Equations (2) and (3) are coupled non-linear equations due to the presence of viscous and Joulean dissipation and it is difficult, in general, to solve analytically. When neglecting the viscous dissipative heating ($N = 0$), equations (2) and (3) become linear and solutions can easily be obtained. It is important to mention here that for $N = 0$, the present problem is exactly the same as discussed by (Jha *et al.*, 2015). However, in many practical applications, N cannot be zero ($N \neq 0$), but in many situations it can take small values. Small value of $N (< 1)$ facilitate finding analytical solutions of equations (2) and (3) by using perturbation method in the form:

$$U(Y) = U_0(Y) + NU_1(Y) + \dots \tag{5}$$

$$\theta(Y) = \theta_0(Y) + N\theta_1(Y) + \dots \tag{6}$$

where the second and higher terms on the right side give a correction to θ_0, U_0 accounting for the dissipative effects. Substituting equations (5) - (6) into equations (2) - (3) and equating like powers of N to zero, we obtain, the zero order equations:

$$\frac{d^2U_0}{dY^2} - M^2U_0 + \theta_0 = 0$$

$$\frac{d^2\theta_0}{dY^2} = 0 \tag{7}$$

with the boundary conditions:

$$U_0(Y) = \beta_v Kn \frac{dU_0}{dY}, \theta_0(Y) = \xi + \beta_v Kn \ln \frac{d\theta_0}{dY} \text{ at } Y=0 \tag{9}$$

$$U_0(Y) = -\beta_v Kn \frac{dU_0}{dY}, \theta_0(Y) = 1 - \beta_v Kn \ln \frac{d\theta_0}{dY} \text{ at } Y=1$$

The first order equations are obtain by equating like powers of N to one, we obtain the first order equations:

$$\frac{d^2U_1}{dY^2} - M^2U_1 + \theta_1 = 0 \tag{10}$$

$$\frac{d^2\theta_1}{dY^2} + M^2U_0^2 + \left(\frac{dU_0}{dY} \right)^2 = 0 \tag{11}$$

with the boundary conditions:

$$U_1(Y) = \beta_v Kn \frac{dU_1}{dY}, \theta_1(Y) = \beta_v Kn \ln \frac{d\theta_1}{dY} \text{ at } Y=0 \tag{12}$$

$$U_1(Y) = -\beta_v Kn \frac{dU_1}{dY}, \theta_1(Y) = -\beta_v Kn \ln \frac{d\theta_1}{dY} \text{ at } Y=1$$

By solving equations (7) and (8), under boundary conditions (9) and (10), we obtained $U_0(Y)$ and $\theta_0(Y)$, respectively, as follows:

$$\theta_0(Y) = A_0 + A_1(Y) \tag{13}$$

$$U_0(Y) = C_1 \cosh(MY) + C_2 \sinh(MY) + \frac{1}{M^2} [A_0 + A_1(Y)] \tag{14}$$

Also, solving equations (11) and (12) under boundary condition (13) and (14), we obtained $U_1(Y)$ and $\theta_1(Y)$, respectively, as follows:

$$\theta_1(Y) = A_{23} \cosh(2MY) + A_{24} \cosh(MY) + A_{25} \sinh(MY) + A_{26} \sinh(2MY) + A_{27} Y \cosh(MY) + A_{28} Y \sinh(MY) + A_{29} Y^4 + A_{30} Y^3 + A_{22} Y^2 + C_3 Y + C_4$$

$$U_1(Y) = C_5 \cosh(MY) + C_6 \sinh(MY) - \frac{A_{23}}{3M^2} \cosh(2MY) + A_{31} Y \sinh(MY) + A_{32} Y \cosh(MY) - \frac{A_{26}}{3M^2} \sinh(2MY)$$

$$- \frac{A_{27}}{3M^2} \sinh(2MY) - \frac{A_{27}}{4M} Y^2 \sinh(MY) - \frac{A_{28}}{4M} Y^2 \cosh(MY) + A_{33} + \left(\frac{A_{29}}{M^2} + A_{34} \right) Y^2 + \frac{A_{30}}{M^2} Y^3 + \frac{C_3}{M^2} Y + \frac{C_4}{M^2}$$

$$\tag{16}$$

The dimensionless rate of heat transfer which is expressed as the Nusselt number can be defined at each boundary, namely as in the following:

$$Nu_0 = \frac{d\theta(0)}{dY} = \frac{d\theta_0(0)}{dY} + N \frac{d\theta_1(0)}{dY}$$

$$Nu_0 = A_1 + NB_{25} \tag{17}$$

while

$$Nu_1 = \frac{d\theta(1)}{dY} = \frac{d\theta_0(1)}{dY} + N \frac{d\theta_1(1)}{dY}$$

$$Nu_1 = A_1 + NB_{26} \tag{18}$$

The dimensionless skin frictions are:

$$\tau_0 = \frac{dU(0)}{dY} = \frac{dU_0(0)}{dY} + N \frac{dU_1(0)}{dY}$$

While

$$\tau_1 = - \frac{dU(1)}{dY} = \left[\frac{dU_0(1)}{dY} + N \frac{dU_1(1)}{dY} \right]$$

where $A_0, A_1, B_1, \dots, B_5$ are all constants given in the Appendix.

RESULTS AND DISCUSSION

Influence of viscous and Joulean dissipation on steady MHD natural convection flow in a vertical

micro-channel in the presence of velocity slip and temperature jump is investigated. The interactive effects of wall-ambient temperature difference ratio (ξ), Knudsen number ($\beta_v Kn$), fluid wall interaction parameter (h), Hartmann number (M) and viscous and Joulean dissipation parameter (N) on the fluid velocity, temperature, skin friction and rate of heat transfer which is expressed as the Nusselt number are computed. The present parametric study has been performed in the continuum and slip flow regimes ($Kn \leq 0.1$). Also, for air and various surfaces, the values of β_v and β_t range from near to and from near to more than , respectively. So, this study has been performed over the reasonable ranges $0 \leq \beta_v Kn \leq 0.1$ of $0 \leq \ln \leq 10$ and [11]. The selected reference values of and for the present analysis are and respectively as given in (Jha *et al.* 2015).

Figures 2 (a, b) displays the combined effects of Hartmann number (M) as well as wall-ambient temperature difference ratio ($\xi = -1$: one heating and one cooling; $\xi = 0$: one heating $\xi = 1$: and one not heating, both walls are heated) on velocity profile. It is interesting to note that, velocity decreases with increasing Hartmann number as well as wall-ambient temperature difference ratio, indicating that an increase in field acts to decrease the influence of dissipation heating on the velocity profiles. Furthermore, any increase in Joulean dissipation accompanying an increase in field is more than overcome by the corresponding decrease in viscous dissipation. This decrease in viscous dissipation is due to the fact that magnetic field tends to flatten the velocity profile as well as decrease the flow.

Figures 3 (a, b, c) show the effects of buoyancy parameter (N) and Hartmann number (M) on velocity profile for different values of wall-ambient temperature difference ratio. It is observed that, increase in buoyancy parameter enhances the fluid velocity. However, it is worth noting that the influence of buoyancy parameter and Hartmann number becomes significantly pronounced in the case of asymmetric heating ($\xi = -1$).

Figure 4 depict the influence of Hartmann number (M) as well as wall-ambient temperature difference ratio on temperature profile. It is observed that, fluid temperature decreases with increasing Hartmann number as well as wall-ambient temperature difference ratio.

Figures 5 (a, b, c) displays the effects of buoyancy parameter (N) and Hartmann number (M) on

temperature profile. It is evident that, the influence of buoyancy parameter is to enhance the fluid temperature while increase in Hartmann number (M) decreases the fluid temperature. Further, the effect of buoyancy parameter as well as Hartmann number on the fluid temperature is pronounced in the case of symmetric heating ($\xi = 1$).

Table I display the impact of viscous dissipation ($N \neq 0$) as well as Hartmann number (M) on the rate of heat transfer at the wall ($Y = 0$) and ($Y = 1$), respectively. As it can be seen from Table I, the rate of heat transfer increases with an increase in buoyancy parameter (N) while, as Hartmann number increases, the impact of buoyancy parameter on the rate of heat transfer decreases. In addition, the effect of viscous dissipation ($N \neq 0$) on the rate of heat transfer is significant in the case of asymmetric heating ($\xi = 0, -1$). Furthermore, in the absence of viscous and Joulean dissipation ($N = 0$), rate of heat transfer is same at both micro-channel walls while it is different in the presence of viscous and Joulean dissipation ($N \neq 0$).

Table II shows the influence of viscous dissipation ($N \neq 0$) as well as rarefaction parameter ($\beta_v Kn$) on the skin friction at the wall ($Y = 0$) and ($Y = 1$), respectively. It is evident from Table, the skin friction increases with an increase in rarefaction parameter and buoyancy parameter (N). In addition, the influence of buoyancy parameter (N) on the skin friction decreases as rarefaction parameter increases.

Conclusion

This study considered the fully developed natural convection flow in a vertical parallel plate micro-channel under the effects of viscous and joulean dissipation. The derivation of the velocity and temperature profile for the existing in Hartmann flow is presented for various Hartmann number when dissipation is not neglected. The effects of Hartmann number, Knudsen number, fluid wall interaction parameter and dissipation parameter on the flow formation as well as rate of heat transfer are demonstrated through graphs and tables. The main findings are:

1. Increase in Hartmann number reduced the influence of viscous as well as joulean dissipation on the velocity, temperature and rate of heat transfer.
2. An increase in field acts to decrease the

influence of dissipation heating on the velocity and temperature profiles.

3. The rate of heat transfer increases with an increase in dissipation parameter

Appendix

$$A_7 = \frac{A_0}{M} + \beta_v Kn M \sinh(M); A_8 = \sinh(M) + \beta_v Kn M \cosh(M); A_9 = -A_4 \beta_v Kn - A_2;$$

$$A_{10} = A_7 A_5 + A_8; A_{11} = A_9 - A_7 A_6; A_{12} = A_{16} = M^2 C_1^2 + M^2 C_2^2; A_{13} = 2M^2 C_1 C_2;$$

$$A_{14} = 2C_1 A_0 + \frac{2A_1 C_2}{M}; A_{15} = 2C_2 A_0 + \frac{2A_1 C_1}{M}; A_{17} = 2C_1 A_1; A_{18} = 2C_2 A_1; A_{19} = \frac{A_1^2}{M^2};$$

$$A_{20} = \frac{2A_0 A_1}{M^2}; A_{21} = \frac{A_0^2}{M^4} + \frac{A_1^2}{M^4}; A_{22} = -\frac{A_{12}}{4} - \frac{A_{21}}{2} + \frac{A_{16}}{4}; A_{23} = -\frac{A_{12}}{8M^2} - \frac{A_{16}}{8M^2};$$

$$A_{24} = -\frac{A_{14}}{M^2} + \frac{2A_{18}}{M^3}; A_{25} = -\frac{A_{15}}{M^2} + \frac{2A_{17}}{M^3}; A_{26} = -\frac{A_{13}}{4M^2}; A_{27} = -\frac{A_{17}}{M^2}; A_{28} = -\frac{A_{18}}{M^2};$$

$$A_{29} = -\frac{A_{19}}{12}; A_{30} = -\frac{A_{20}}{6}; A_{31} = \frac{A_{28}}{4M^2} - \frac{A_{24}}{2M}; A_{32} = \frac{A_{27}}{4M^2} - \frac{A_{25}}{2M}; A_{33} = \frac{24A_{29}}{M^6} + \frac{2A_{22}}{M^4};$$

$$A_{34} = \frac{12A_{29}}{M^4} + \frac{A_{22}}{M^4}; B_1 = A_{23} + A_{24};$$

$$B_2 = A_{23} \cosh(2M) + A_{24} \cosh(M) + A_{25} \sinh(M) + A_{26} \sinh(2M) + A_{27} \cosh(M) + A_{28} \sinh(M) + A_{29} + A_{30}$$

$$B_3 = -\frac{A_{13}}{2M} - \frac{A_{15}}{M} + \frac{A_{17}}{M^2};$$

$$B_4 = -\frac{A_{12}}{2} - \frac{A_{12}}{4M} \sinh(2M) - \frac{A_{11}}{2M} \cosh(2M) - \frac{A_{14}}{M} \sinh(M) - \frac{A_{15}}{M} \cosh(M) - \frac{A_{16}}{4M} \sinh(2M) + \frac{A_{16}}{2} - \frac{A_{17}}{M} \sinh(M) + \frac{A_{17}}{M^2} \cosh(M) - \frac{A_{18}}{M} \cosh(M) - \frac{A_{18}}{M^2} \sinh(M) - \frac{A_{19}}{3} - \frac{A_{19}}{3} - A_{21} + C_3;$$

$$B_5 = \beta_v Kn \ln; B_6 = \beta_v Kn \ln B_3 - B_1; B_7 = 1 + \beta_v Kn \ln; B_8 = -\beta_v Kn \ln B_4 - B_2; B_9 = B_7 + B_5;$$

$$B_{10} = B_8 - B_6; B_{11} = A_{33} - \frac{A_{23}}{3M^2};$$

$$B_{12} = \frac{A_{23}}{3M^2} \cosh(2M) + A_{31} \sinh(M) + A_{32} \cosh(M) - \frac{A_{26}}{3M^2} \sinh(2M) - \frac{A_{27}}{4M} \sinh(M) - \frac{A_{28}}{4M} \cosh(M) + A_{33} + \frac{A_{29}}{M^2} + \frac{A_{30}}{M^2} + \frac{6A_{30}}{M^4} + \frac{C_3}{M^2} + \frac{C_4}{M^2};$$

$$B_{13} = -\frac{A_{25}}{2M} - \frac{2MA_{26}}{3M^2} + \frac{A_{27}}{4M^2} + \frac{6A_{30}}{M^4} + \frac{C_3}{M^2};$$

$$B_{14} = -\frac{2A_{23}}{3M} \sinh(2M) - \frac{A_{24}}{2M} \sinh(M) - \frac{A_{24}}{2} \cosh(M) - \frac{A_{25}}{2M} \cosh(M) - \frac{A_{25}}{2} \sinh(M) - \frac{2A_{26}}{3M} \cosh(2M)$$

$$B_{15} = \frac{A_{27}}{4M^2} \cosh(M) + \frac{A_{27}}{4M} \sinh(M) - \frac{A_{27}}{2M} \sinh(M) - \frac{A_{27}}{4} \cosh(M) + \frac{A_{28}}{4M^2} \sinh(M)$$

$$B_{16} = \frac{A_{28}}{4M} \cosh(M) - \frac{A_{28}}{2M} \cosh(M) - \frac{A_{28}}{4} \sinh(M) + \frac{24A_{29}}{M^4} + \frac{4A_{29}}{M^2} + \frac{6A_{30}}{M^4} + \frac{3A_{30}}{M^2} + \frac{2A_{32}}{M^2} + \frac{C_3}{M^2};$$

$$B_{17} = B_{14} + B_{15} + B_{16}; B_{18} = \beta_v Kn M; B_{19} = \beta_v Kn B_{13} - \frac{C_4}{M^2} - B_{11};$$

$$B_{20} = \cosh(M) + \beta_v Kn M \sinh(M); B_{21} = \sinh(M) + \beta_v Kn M \cosh(M); B_{22} = -B_{17} \beta_v Kn - B_{12};$$

$$B_{23} = B_{21} + B_{18} B_{20}; B_{24} = B_{22} - B_{19} B_{20}; B_{25} = A_{25} M + 2A_{26} M + A_{27} + C_3;$$

$$B_{26} = 2A_{23} M \sinh(2M) + A_{24} M \sinh(M) + A_{25} M \cosh(M) + 2A_{26} M \cosh(2M) + A_{27} \cosh(M) + A_{28} \sinh(M) + A_{28} M \sinh(M) + 4A_{29} + 3A_{30} + 2A_{22} + C_3;$$

$$C_1 = A_6 + C_2 A_5; C_2 = \frac{A_{11}}{A_{10}}; C_3 = \frac{B_{10}}{B_9}; C_4 = B_6 + C_3 B_5; C_5 = B_{19} + C_6 B_{18}; C_6 = \frac{B_{24}}{B_{23}}$$

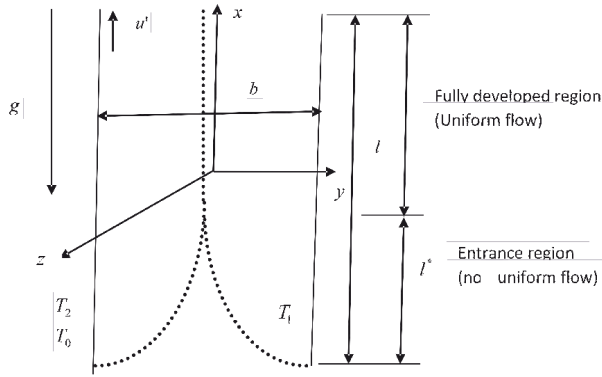


Figure 1: Schematic diagram

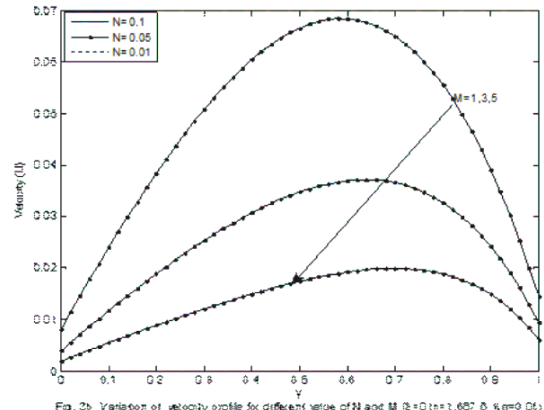


Fig. 2b: Variation of velocity profile for different value of N and M ($\xi=0, \eta=1, \beta_1=0, \beta_2=0, K=0$)

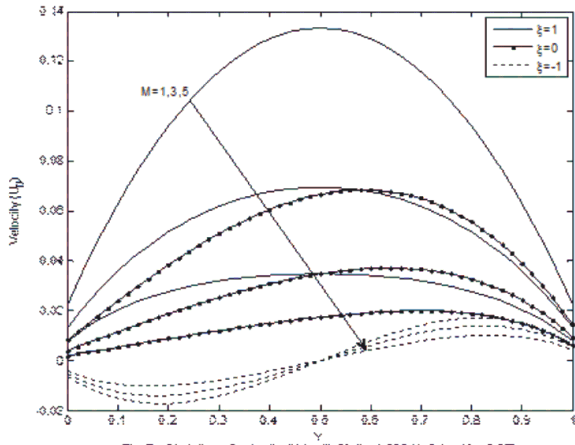


Fig. 2a: Variation of velocity (U_y) with M ($\eta=1, \beta_1=0, \beta_2=0, K=0, N=0.05$)

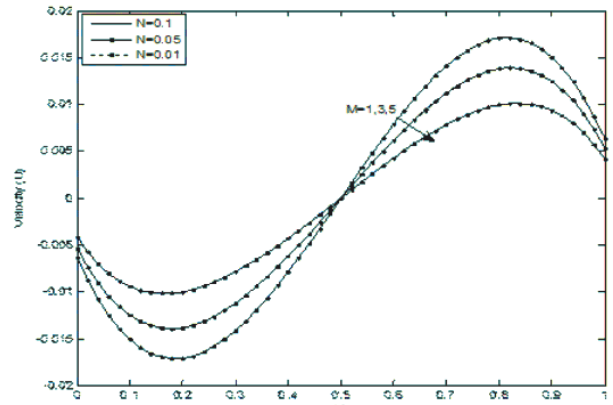


Fig. 3c: Variation of velocity profile for different value of N and M ($\xi=-1, \eta=1, \beta_1=0, \beta_2=0, K=0.05$)

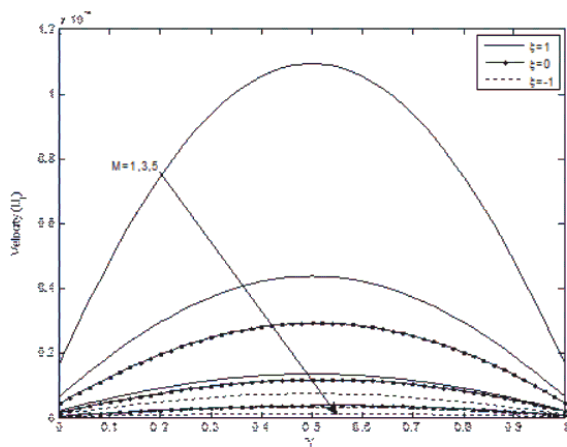


Fig. 2b: Variation of velocity (U_y) with M ($\eta=1, \beta_1=0, \beta_2=0, K=0.05$)

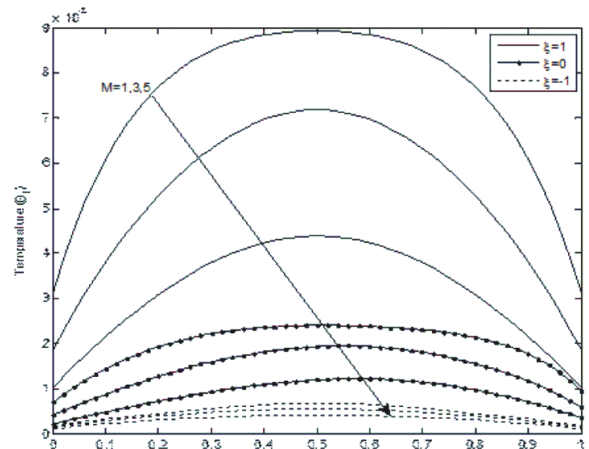


Fig. 4: Variation of temperature (T) with M ($N=0, \eta=1, \beta_1=0, \beta_2=0, K=0.05$)

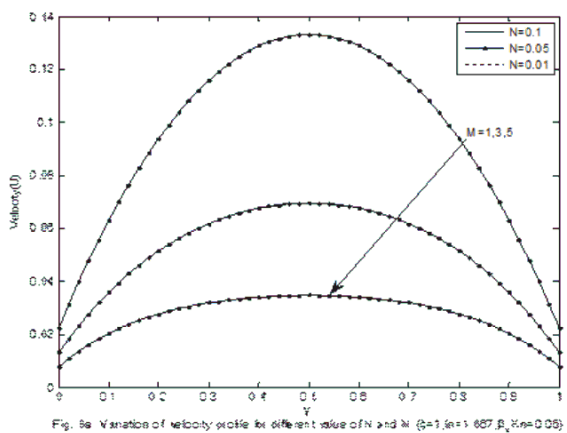


Fig. 5a: Variation of velocity profile for different value of N and M ($\xi=1, \eta=1, \beta_1=0, \beta_2=0, K=0.05$)

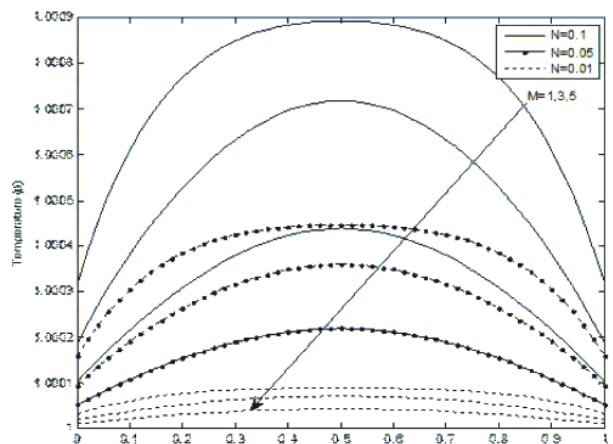


Fig. 6a: Variation of temperature profile for different value of N and M ($\xi=1, \eta=1, \beta_1=0, \beta_2=0, K=0.05$)

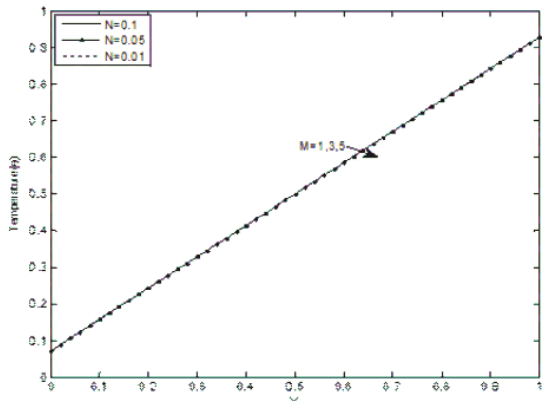


Fig. 5b: Variation of temperature profile for different value of M and N ($\beta=0.001, \beta_0=1.027, \beta_1, Kn=0.05$)

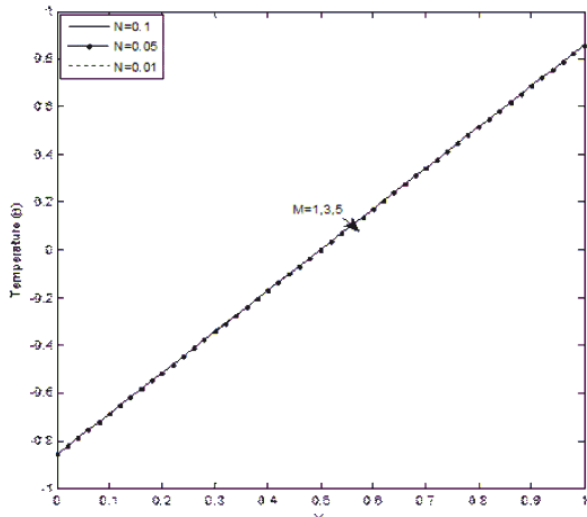


Fig. 5c: Variation of temperature profile for different value of N and M ($\beta=-1, \beta_0=1.027, \beta_1, Kn=0.05$)

Table 1: Numerical values of rate of heat transfer on the vertical micro-channel walls

M	N	$\xi = 1$		$\xi = 0$		$\xi = -1$	
		Nu_0	Nu_1	Nu_0	Nu_1	Nu_0	Nu_1
1.0	0.01	0.00038	-0.00038	0.85720	0.85700	1.71426	1.71422
	0.05	0.00190	-0.00191	0.85754	0.85754	1.71434	1.71413
	0.1	0.00381	-0.00381	0.85797	0.85796	1.71444	1.71403
3.0	0.01	0.00022	-0.00022	0.85717	0.85705	1.71425	1.71421
	0.05	0.00112	-0.00112	0.85737	0.85676	1.71432	1.71420
	0.1	0.00225	-0.00225	0.85762	0.85640	1.71441	1.71406
5.0	0.01	0.00012	-0.00012	0.85715	0.85708	1.71425	1.71422
	0.05	0.00062	-0.00062	0.85725	0.85691	1.71431	1.71417
	0.1	0.00124	-0.00124	0.85739	0.85670	1.71437	1.71410

Table 2: Numerical values of skin friction on the vertical micro-channel walls

M	N	$\xi = 1$		$\xi = 0$		$\xi = -1$	
		τ_0	τ_1	τ_0	τ_1	τ_0	τ_1
1.0	0.01	0.45171	-0.45171	0.16245	-0.28925	-0.12681	-0.12681
	0.05	0.45184	-0.45184	0.16248	-0.29828	-0.12679	-0.12682
	0.1	0.45202	-0.45202	0.16252	-0.28934	-0.12679	-0.12683
3	0.01	0.26566	-0.26566	0.07914	-0.18652	-0.10737	-0.10738
	0.05	0.26571	-0.26571	0.07915	-0.18653	-0.10738	-0.10738
	0.1	0.26578	-0.26578	0.07917	-0.18655	-0.10738	-0.10739
5	0.01	0.15829	-0.15829	0.03718	-0.12110	-0.08392	-0.08392
	0.05	0.15830	-0.15830	0.03719	-0.12111	0.008391	-0.08392
	0.1	0.15832	-0.15832	0.03719	-0.12111	0.08391	-0.08392

REFERENCES

Basant K. Jha and Babatunde Aina, Impact of Viscous Dissipation on Fully Developed Natural Convection Flow in a Vertical Micro-Channel, *Journal of Heat Transfer*, 2018, DOI:10.1115/1.4039641

Eckert, E. R. G., and Drake, R. M., Jr. Analysis of Heat and Mass Transfer, McGraw-Hill, New York, 1972: Chap. 11.

Fletcher J. O. and Frederick J. Y., Natural convection between heated vertical plates inn a horizontal magnetic field, *Fluid Mech.* 1961, 512-518

Goniak R., and Duffa G. “Corrective Term in Wall Slip Equations for Knudsen Layer” *J. Thermophys. Heat Transfer*, 1995; 9: 383-384.

Jha, B. K., Aina, Babatunde and Ajiya A. T., MHD Natural Convection Flow in a Vertical Parallel Plate Microchannel, *Ain Shams Engineering Journal*, 2015, Vol. 6, pp 289-295.

Jha, B. K., Aina, Babatunde and Ajiya A. T., Role of Suction/Injection on MHD Natural Convection Flow in a Vertical Microchannel, *International Journal of Energy & Technology* 2015, Vol. 7, pp 30-39.

Jha, B. K., Aina, Babatunde and Sani Isa, Fully Developed MHD Natural Convection Flow in a Vertical Annular Microchannel: An exact solution, *Journal of King Saud university- Science*, 2015, 27, pp 253-259

Jha, B. K., Aina, Babatunde and Sani Isa, Transient Magnetohydrodynamic Free Convective Flow in Vertical Micro-Concentric-Annuli, Proc IMechE Part N: *J Nanoengineering and Nanosystems*, DOI: 10.1177/1740349915578956

Jha, B. K., and Babatunde Aina, MHD Natural Convection Flow in a Vertical Micro-Porous- Annulus in the Presence of Radial Magnetic Field, *Journal of Nanofluids*, 2016, doi:10.1166/jon.2016.1204

- Jha, B. K., Babatunde Aina and Sani Isa, MHD Natural Convection flow in a Vertical Micro-Concentric-Annuli in the Presence of Radial Magnetic Field: An Exact Solution, *Journal of Ain Shams Engineering*, 2015, <http://dx.doi.org/10.1016/j.asej.2015.07.010>
- Sheikholeslami M., CuO-water nanofluid free convection in a porous cavity considering Darcy law, *Eur. Phys. J. Plus* (2017)132:55
- Sheikholeslami M., Influence of Lorentz forces on nanofluid flow in a porous cavity by means of non- Darcy mode, Vol. 34 Issue: 8, pp.2651-2667, <https://doi.org/10.1108/EC-01-2017-0008>
- Sheikholeslami M., Influence of magnetic field on nanofluid free convection in an open porous cavity by means of Lattice Boltzmann method, *Journal of molecular liquids*, 234 (2017) 364-374
- Sheikholeslami M., Numerical investigation for CuO-H₂O nanofluid flow in a porous channel with magnetic field using mesoscopic method, *Journal of molecular liquids*, 249 (2018) 739-746
- Sheikholeslami M., Shamlooei M and Moradi R., Fe₃O₄-Ethylene glycol nanofluid forced convection inside a porous enclosure in existence of Coulomb force, *Journal of molecular liquids*, 249 (2018) 429-437
- Sheikholeslami Mohsen, Numerical investigation of nanofluid free convection under the influence of electric field in a porous enclosure, *Journal of molecular liquids*, 249 (2018) 1212-1221
- Sheikholeslamia M and Shehzad S.A., Simulation of water based nanofluid convective flow inside a porous enclosure via non-equilibrium model, *International Journal of Heat and Mass Transfer* 120 (2018) 1200–1212
- Sheikholeslamia Mohsen and Houman B. Rokni, Numerical simulation for impact of Coulomb force on nanofluid heat transfer in a porous enclosure in presence of thermal radiation, *International Journal of Heat and Mass Transfer* 118 (2018) 823–831
- Sheikholeslamia Mohsen and Seyednezhad Mohadeseh, Simulation of nanofluid flow and natural convection in a porous media under the influence of electric field using CVFEM, *International Journal of Heat and Mass Transfer* 120 (2018) 772–781
- Sheikholeslamia Mohsen and Shehzad S.A., Numerical analysis of Fe₃O₄–H₂O nanofluid flow in permeable media under the effect of external magnetic source, *International Journal of Heat and Mass Transfer* 118 (2018) 182–192
- Umavathi J. C. and Chamkha A. J. Combined effect of variable viscosity and thermal conductivity on free convection flow of a viscous fluid in a vertical channel, *International journal of numerical methods for heat and fluid flow*, 2016, 26(1), pp. 18-39